Role and contribution of the resonance effect for the decay process of $\bar{B}_s^0 \to \pi^+\pi^- P^*$

Xi-Liang Yuan (原喜亮)[1†] Chao Wang (王超)[1‡] Zhuang-Dong Bai (白壮东)[1§] Gang Lü (吕刚)[2¶]

[1]School of Ecology and Environment, Northwestern Polytechnical University, Xi'an 710072, China
[2]Institute of Theoretical Physics, College of Physics, Henan University of Technology, Zhengzhou 450001, China

Abstract: The magnitude of the direct CP asymmetry generated during the weak decay of hadrons is attributed to the weak phase and certain strong phases. The weak phase originates from the CKM matrix, while a strong phase may result from the resonance effect produced by the mixing of vector mesons $V\left\{\rho^0(770), \omega(782), \phi(1020)\right\}$ to $\pi^+\pi^-$ meson pairs. $\rho^0(770)$ can decay directly into $\pi^+\pi^-$ meson pairs; both $\omega(782)$ and $\phi(1020)$ can also decay into $\pi^+\pi^-$ meson pairs, with a small contribution from isospin symmetry breaking. The main contribution for the middle state vector meson $\rho^0(770)-\omega(782)-\phi(1020)$ interference is the mix of $\rho^0(770)$, $\omega(782)-\rho^0(770)$, and $\phi(1020)-\rho^0(770)$. We calculated the CP asymmetry and decay branching ratio for $\bar{B}_s^0 \to \pi^+\pi^-\pi^0(\bar{K}^0)$within the framework of QCD factorization and compared them with previous studies. We also analyzed the $\bar{B}_s^0 \to \pi^+\pi^-\eta(\eta^{(\prime)})$ decay process. The results show that the CP asymmetry of these four decay processes is significantly enhanced, especially for the $\bar{B}_s^0 \to \pi^+\pi^-\bar{K}^0$ decay process. Moreover, the decay branching ratio also changes under the resonance effect. These results might provide support for the experimental analysis of the $\bar{B}_s^0$ meson.

Keywords: CP asymmetry, QCD factorization, resonance effect

DOI: 10.1088/1674-1137/ade6d8 **CSTR:** 32044.14.ChinesePhysicsC.49113103

I. INTRODUCTION

The non-leptonic decay of hadrons containing heavy quarks plays a crucial role in testing the Standard Model (SM) by examining the charge parity (CP) asymmetry mechanism in flavor physics [1, 2]. It can also enhance our understanding of Quantum Chromodynamics and help in discovering new physical phenomena beyond the SM. The result of CP asymmetry is related to the weak phase in the Cabibbo-Kobayashi-Maskawa (CKM) matrix, which describes the mixing of quarks from different generations. In addition, a strong phase is also required to observe CP asymmetries [3]. Typically, this strong phase is provided by several phenomenological models and QCD loop corrections. Similarly, the generation of these phases may affect the decay process of vector mesons, CP asymmetries, and even decay branching ratios. Recently, attention on CP asymmetry and the decay branching ratio in the B meson system has increased in both theoretical and experimental terms. The study of B meson decays has gradually shifted from the analysis of two-body decays to the analysis of three-body decays, which has been widely carried out [4−6]. In recent years, the BABAR, Belle, and LHCb collaborations have measured various CP asymmetry and branching ratio parameters for three-body charmless B decays in experiments [7−9]. In theory, a fully developed and widely used approach has been established to calculate the hadron matrix elements of B meson non-leptonic weak decay. It includes naive factorization [10, 11], QCD factorization (QCDF) [12−14], perturbative QCD (PQCD) [15−17] approaches, soft collinear efficient theory (SCET) [18, 19], and factorization assisted topological-amplitude approach (FAT) [20−22].

Inspired by the achievements on two-body B decays, we followed a quasi-two-body approach in this study to

Received 27 April 2025; Accepted 17 June 2025; Published online 18 June 2025

* Supported by National Natural Science Foundation of China (Project No.11805153) and Natural Science Foundation of Henan Province (Project No.252300420319)

† E-mail: xiliangyuan18@sina.com
‡ E-mail: chaowang@nwpu.edu.cn (Corresponding author)
§ E-mail: baizhuangdong@163.com
¶ E-mail: ganglv66@sina.com (Corresponding author)

calculate the three-body decay process of the B meson under the resonant effect. The vector resonant effects are described using the common Breit-Wigner formalism, and a strong coupling is used to explain the subsequent two-body decay of the vector meson. Under the resonance contribution, the vector meson dominance model (VMD) predicts that the vacuum polarization of the photon is entirely composed of vector mesons of $\rho^0(770)$, $\omega(782)$, and $\phi(1020)$ [23]. The transitions of $\omega(782)$ and $\phi(1020)$ decay into $\pi^+\pi^-$ meson pairs, which originate from isospin breaking related to the mixings of $\omega(782)-\rho^0(770)$ and $\phi(1020)-\rho^0(770)$. Given that the decay rate of $\rho^0(770)\to\pi^+\pi^-$ is 100% [24], the mixing of intermediate particles $\rho^0(770)$, $\omega(782)-\rho^0(770)$, and $\phi(1020)-\rho^0(770)$ is mainly considered in our theory, ignoring the interference from other processes. In addition, the strong phase from the three-body decay can be produced by intermediate resonance hadrons associated with the Breit-Wigner form. A new strong phase is formed through the mixing of the intermediate resonance hadrons and is combined with the weak phase calculated from the CKM matrix. We propose a matrix composed of hadrons to connect the intermediate state of the decay process with the physical state of the isospin state [25]. The interference caused by the three mesons, namely $\rho^0(770)$, $\omega(782)$, and $\phi(1020)$, can be solved by dynamical mechanisms. The analysis of vector meson resonance has greatly contributed to the understanding of particle properties and meson interactions [26].

In previous calculations of CP asymmetry theory, we investigated the non-leptonic decay processes of $\bar{B}_s^0\to\rho^0(770)\pi^0(\bar{K}^0)\to\pi^+\pi^-\pi^0(\bar{K}^0)$ with the interference using PQCD [27]. The PQCD approach incorporates QCD corrections owing to transverse momentum and introduces the Sudakov factor to suppress non-perturbative effects. Endpoint divergence is regulated by including the parton transverse momentum k_T and Sudakov factor at the expense of modeling the additional k_T dependence of meson wave functions. Annihilation corrections are included. The non-perturbative contribution is contained in the hadron wave function. In the latest theoretical calculations of the decay branching ratio, in addition to the PQCD approach, the FAT approach is also introduced [28], which includes the non-perturbation and non-factorization contributions of two-body B decays. The decay amplitude of two-body charmless B decay is divided into different electroweak topological Feynman figures under $SU(3)$ symmetry. By globally fitting all experimental data for these decays, the topological amplitudes, including the nonfactorizable QCD contributions, are extracted. However, the precision of this topological approach is limited by the size of the $SU(3)$ breaking effect.

In this study, we applied the QCDF approach to study and compare the results of new calculations with previous ones, and to assess the accuracy of the theoretical QCD calculations. We extended the two-body decay framework to describe the three-body decay process under QCDF, where the strong interaction is divided into a hard scattering part (perturbative calculation) and a non-perturbative part involving light components (such as the form factor and light cone distribution amplitude). For three-body decay, we considered the case of a cascade decay via two-body decays ($B\to VP\to\pi^+\pi^-P$) by a quasi-two-body approximation, thus preserving the framework of QCDF, which assumes that ρ is on-shell. The processes were decomposed into $B\to VP$ and $V\to\pi^+\pi^-$. The resonance effect was introduced using the Breit-Wigner form. When we calculated the CP asymmetry and branching ratio, the three-body phase space integration was converted to integration over the intermediate state invariant mass $s=m^2_{\pi^+\pi^-}$, and the resonance region $s\sim m_\rho^2$ was assumed to dominate the contribution. At this point, the hard scattering part of the QCDF depends only on s, while the non-perturbative part remains in the same form as that of the two-body decay. Within the framework of the QCDF, the analysis of the B meson decay can set the b-quark mass to infinity and ignore the higher-order contribution of $1/m_b$; the two-body non-lepton decay amplitude can be expressed as the product of the form factor from the initial to final mesons and the light cone distribution amplitude of the final meson in the heavy quark limit. When $m_b\to\infty$, $1/m_b$ becomes negligible; thus, the contribution of $1/m_b$ power corrections is not considered. The logarithmically divergent integral is usually parameterized in a model-independent manner and explicitly expressed as $\int_0^1 \mathrm{d}x/x\to \mathrm{X}_A$ [29]. We calculated the CP asymmetry result of $\bar{B}_s^0\to V(\rho^0(770),\omega(782),\phi(1020))\pi^0(\bar{K}^0)\to\pi^+\pi^-\pi^0(\bar{K}^0)$ decay process and compared the influence of PQCD and QCDF on CP asymmetry under the resonance effect. CP asymmetry and local integration results of the two attenuation processes of $\bar{B}_s^0\to V(\rho^0(770),\omega(782),\phi(1020))\eta(\eta')\to\pi^+\pi^-\eta(\eta')$ were also obtained. Subsequently, we calculated the decay branching ratio of these four decay processes under the resonance effect and the decay branching ratio without the resonance effect and compared these results with the latest theoretical results. The PQCD approach provides results only for the direct decay process, while the branching ratios of three-body B decays studied under the FAT approach consider the virtual effects of intermediate resonances $\rho^0(770)$, $\omega(782)$, $\phi(1020)$ on quasi-two-body decays. We compared and analyzed these results as well. We also explored the role and contribution of resonance effects on the decay process $\bar{B}_s^0\to\pi^+\pi^-P$.

The overall structure of this paper is as follows. In Section II, we introduce the resonance mechanism in Subsection A, briefly explain the QCDF approach in Subsection B, and present the amplitude involving the $\rho^0(770)$, $\omega(782)$, and $\phi(1020)$ interferences in Subsection

C. Then, in Section III, we present the computational and local integral forms of the CP asymmetry as well as the branching ratios of the three-body decay process in Subsections A, B, and C, respectively. In Section IV, we analyze the curve results of CP asymmetry in these decay processes and calculate the local integral CP asymmetry and decay branching ratios in different phase space regions. Conclusions are presented in Section V.

II. CALCULATION OF AMPLITUDE UNDER QCDF

A. Introduction of resonance mechanism

According to the vector meson dominance model (VMD), e^+e^- can annihilate into a photon γ, whose vacuum polarization is dressed by coupling vector mesons $\rho^0(770)$, $\omega(782)$, and $\phi(1020)$. These vector mesons can then decay into $\pi^+\pi^-$ meson pairs. The VMD successfully describes the interaction between photons and hadrons [23]. The $\rho^0(770)-\omega(782)-\phi(1020)$ interferences are caused by the difference in quark mass and electromagnetic interaction effects; they can decay directly into $\pi^+\pi^-$ meson pairs. Besides, the transitions of $\omega(782)$ and $\phi(1020)$ decay into $\pi^+\pi^-$ meson pairs, which originate from isospin breaking related to the mixing of $\omega(782)-\rho^0(770)$ and $\phi(1020)-\rho^0(770)$ [25]. We establish a resonance effect by considering the interference caused by the mixing of three intermediate state particles ($\rho^0(770)$, $\omega(782)$, $\phi(1020)$). Given that the resonance effect is not a physical representation, a matrix is constructed to transform the isospin field into a physical representation. The relationship between the isospin field (ρ_I,ω_I,ϕ_I) and physical representation (ρ,ω,ϕ) can be described by the matrix, while ignoring the contribution of higher order terms. To facilitate readability, we use ρ,ω, and ϕ to represent $\rho^0(770)$, $\omega(782)$, and $\phi(1020)$, respectively. It can be expressed as

$$\begin{pmatrix}\rho\\ \omega\\ \phi\end{pmatrix} = \begin{pmatrix}\langle\rho_I|\rho\rangle & \langle\omega_I|\rho\rangle & \langle\phi_I|\rho\rangle\\ \langle\rho_I|\omega\rangle & \langle\omega_I|\omega\rangle & \langle\phi_I|\omega\rangle\\ \langle\rho_I|\phi\rangle & \langle\omega_I|\phi\rangle & \langle\phi_I|\phi\rangle\end{pmatrix}$$

$$\begin{pmatrix}\rho_I\\ \omega_I\\ \phi_I\end{pmatrix} = \begin{pmatrix}1 & -F_{\rho\omega}(s) & -F_{\rho\phi}(s)\\ F_{\rho\omega}(s) & 1 & -F_{\omega\phi}(s)\\ F_{\rho\phi}(s) & F_{\omega\phi}(s) & 1\end{pmatrix}, \quad (1)$$

where $F_{VV}(s)(V=\rho,\omega,\phi)$ is of order $O(\lambda)$, $(\lambda \ll 1)$ [25]. Based on the isospin field $\rho_I(\omega_I,\phi_I)$, we can construct the isospin basis vectors $|I,I_3\rangle$, where I and I_3 are the isospin and its third components, respectively. Thus, physical states can be represented as linear combinations of basis vectors in a matrix. We used orthogonal normalization to obtain the relationship between the physical state of the particle and the isospin basis vector. Thus, the physical manifestation of this form can be clearly expressed as $\rho=\rho_I-F_{\rho\omega}(s)\omega_I-F_{\rho\phi}(s)\Phi_I$, $\omega=F_{\rho\omega}(s)\rho_I+\omega_I-F_{\omega\phi}(s)\Phi_I$, $\Phi=F_{\rho\phi}(s)\rho_I+F_{\omega\phi}(s)\omega_I+\Phi_I$.

Considering the physical and isospin representations, we define the propagators as $D_{V_1V_2}=\langle 0|TV_1V_2|0\rangle$ and $D^I_{V_1V_2}=\langle 0|TV_1^IV_2^I|0\rangle$, respectively. V_1 and V_2 of $D_{V_1V_2}$ refer to any two of the three particles ρ, ω, and ϕ in physical fields. Incorporating ρ,ω,ϕ from the physical fields into the definition of $D_{V_1V_2}$, we found that the forms $D_{\rho\omega}$, $D_{\rho\phi}$, and $D_{\omega\phi}$ are identical. Given that there is no mixing of three vector mesons in the physical representation, $D_{V_1V_2}$ is equal to zero. We deduced these processes about propagators in detail in a previous theory [29]. In addition, according to the physical state expression of the two-vector meson mixing, the parameters of $F_{\rho\omega}$ are of the order of $O(\lambda)$ $(\lambda \ll 1)$. Given that the multiplication of multiple terms in the equation represents a higher-order term, its effect is suppressed and can be neglected. In this study, we only considered the process involving ρ because the CP asymmetry of $\pi^+\pi^-$ meson pairs produced by the mixing process of ω and ϕ is almost absent under the resonance effect. We can define new mixing parameters based on decay width and mass [30]:

$$\begin{aligned}\Pi_{\rho\omega} &= F_{\rho\omega}(s-m_\rho^2+\mathrm{i}m_\rho\Gamma_\rho)-F_{\rho\omega}(s-m_\omega^2+\mathrm{i}m_\omega\Gamma_\omega),\\ \Pi_{\rho\phi} &= F_{\rho\phi}(s-m_\rho^2+\mathrm{i}m_\rho\Gamma_\rho)-F_{\rho\phi}(s-m_\phi^2+\mathrm{i}m_\phi\Gamma_\phi),\end{aligned} \quad (2)$$

where Γ_V and m_V represent the decay width and mass of vector mesons V $(V=\rho,\omega,\phi)$, respectively. The propagator s_V of vector meson is associated with the invariant mass $\sqrt{s}$, which can be expressed as $s_V=s-m_V^2+\mathrm{i}m_V\Gamma_V$. The vector resonance $\Gamma_V(s)$ for the energy-dependent width can be expressed as [31]

$$\Gamma_V(s)=\Gamma_0\left(\frac{q}{q_0}\right)^3\left(\frac{m_V}{\sqrt{s}}\right)X^2(qr_{BW}), \quad (3)$$

where the expression for the Blatt-Weisskopf barrier factor $X^2(qr_{BW})$ is $\sqrt{\left[1+(q_0r_{BW})^2\right]/\left[1+(qr_{BW})^2\right]}$, $q=\frac{1}{2}\sqrt{\left[s-(m_{\pi^+}+m_{\pi^-})^2\right]\left[s-(m_{\pi^+}-m_{\pi^-})^2\right]/s}$ is the momentum of the final state π^+ or π^- in the rest frame of the resonance V, and q_0 is the value of q when $s=m_V^2$. The value of the barrier radius r_{BW} is 4.0 $(\mathrm{GeV})^{-1}$ for all resonances [32]. In this study, we considered the vector resonance state for the full width value Γ_0, which comes from the fact that PDG of the decay fractions for ρ into $\pi^+\pi^-$ is

100%, with the full width of ρ being 149.1 ± 0.8 MeV; ω into $\pi^+\pi^-$ is $1.53^{+0.11}_{-0.13}$%, with the full width of ω being 8.68 ± 0.13 MeV; and ϕ into $\pi^+\pi^-$ is $(7.3\pm1.3)\times10^{-5}$%, with the full width of ϕ being 4.249 ± 0.013 MeV [24, 33]. These data were also used in subsequent calculations of the decay width.

In addition, the mixing parameters of $\omega-\rho$ and $\phi-\rho$ were extracted from the $e^+e^-\to\pi^+\pi^-$ experimental data [34, 35]. To better interpret the mixing of $\omega-\rho$ and $\phi-\rho$, we define

$$\widetilde{\Pi}_{\rho\omega}=\frac{(s-m_\rho^2+\mathrm{i}m_\rho\Gamma_\rho)\Pi_{\rho\omega}}{(s-m_\rho^2+\mathrm{i}m_\rho\Gamma_\rho)-(s-m_\omega^2+\mathrm{i}m_\omega\Gamma_\omega)},$$
$$\widetilde{\Pi}_{\rho\phi}=\frac{(s-m_\rho^2+\mathrm{i}m_\rho\Gamma_\rho)\Pi_{\rho\phi}}{(s-m_\rho^2+\mathrm{i}m_\rho\Gamma_\rho)-(s-m_\phi^2+\mathrm{i}m_\phi\Gamma_\phi)}. \tag{4}$$

The mixing parameter, including both resonant and non-resonant contributions, depends on the momentum. Moreover, it absorbs the direct decay processes $\omega\to\pi^+\pi^-$ and $\phi\to\pi^+\pi^-$ from the isospin symmetry breaking effect, which are obtained from sources unrelated to the studied decays. The mixing parameters of $\widetilde{\Pi}_{\rho\omega}(s)$ and $\widetilde{\Pi}_{\rho\phi}(s)$ describe the momentum dependence of $\omega-\rho$ and $\phi-\rho$ interferences, respectively [36]. They were fitted by Gardner and O'Connell [37, 38] and measured by Wolfe and Maltman [35, 36]. $\widetilde{\Pi}_{\rho\omega}(s)$ and $\widetilde{\Pi}_{\rho\phi}(s)$ can be expressed in the form of real and imaginary parts:

$$\widetilde{\Pi}_{\rho\omega}(s)=\Re\mathrm{e}\widetilde{\Pi}_{\rho\omega}(m_\omega^2)+\Im\mathrm{m}\widetilde{\Pi}_{\rho\omega}(m_\omega^2),$$
$$\widetilde{\Pi}_{\rho\phi}(s)=\Re\mathrm{e}\widetilde{\Pi}_{\rho\phi}(m_\phi^2)+\Im\mathrm{m}\widetilde{\Pi}_{\rho\phi}(m_\phi^2). \tag{5}$$

Numerical results for the real and imaginary parts of the $\omega-\rho(\phi-\rho)$ mixing parameter $\widetilde{\Pi}_{\rho\omega}(\widetilde{\Pi}_{\rho\phi})$ at $s=m_\omega^2$ $(s=m_\phi^2)$ are as follows [36]:

$$\Re\mathrm{e}\widetilde{\Pi}_{\rho\omega}(m_\omega^2)=-4760\pm440\ \mathrm{MeV}^2,$$
$$\Im\mathrm{m}\widetilde{\Pi}_{\rho\omega}(m_\omega^2)=-6180\pm3300\ \mathrm{MeV}^2;$$
$$\Re\mathrm{e}\widetilde{\Pi}_{\rho\phi}(m_\phi^2)=796\pm312\ \mathrm{MeV}^2,$$
$$\Im\mathrm{m}\widetilde{\Pi}_{\rho\phi}(m_\phi^2)=-101\pm67\ \mathrm{MeV}^2. \tag{6}$$

B. QCD factorization

Beneke et al. argued that the form factor for B to final hadron transition is mainly contributed by the non-perturbative region. The non-factorization effect of hadron matrix elements primarily arises from the exchange of hard gluons in the two-body non-light decay of the B meson. They proposed a new approach for computing hadron matrix elements known as QCD factorization [12, 39]. The low energy effective Hamiltonian form for the non-light and weak decay of B meson decays can be expressed as [40, 41]

$$\mathcal{H}_{\mathrm{eff}}=\frac{G_F}{\sqrt{2}}\sum_{q=u,c}V_q\Big\{C_1(\mu)Q_1^q(\mu)+C_2(\mu)Q_2^q(\mu)+\sum_{k=3}^{10}C_K(\mu)Q_K(\mu)+C_{7\gamma}(\mu)Q_{7\gamma}(\mu)+C_{8g}(\mu)Q_{8g}(\mu)\Big\}+\mathrm{H.c.}, \tag{7}$$

where V_q is the factor associated with the CKM matrix element. The Wilson parameter C_i can be calculated using perturbation theory and renormalization group approaches. Q_i is a valid operator for localization [41]:

the current-current operator is expressed as follows:

$$Q_1^u=(\bar{u}_\alpha b_\alpha)_{V-A}(\bar{q}_\beta u_\beta)_{V-A},\quad Q_1^c=(\bar{c}_\alpha b_\alpha)_{V-A}(\bar{q}_\beta c_\beta)_{V-A},$$
$$Q_2^u=(\bar{u}_\alpha b_\beta)_{V-A}(\bar{q}_\beta u_\alpha)_{V-A},\quad Q_2^c=(\bar{c}_\alpha b_\beta)_{V-A}(\bar{q}_\beta c_\alpha)_{V-A}, \tag{8}$$

the QCD penguins operator is expressed as follows:

$$Q_3=(\bar{q}_\alpha b_\alpha)_{V-A}\sum\nolimits_{q'}(\bar{q}'_\beta q'_\beta)_{V-A},$$
$$Q_4=(\bar{q}_\beta b_\alpha)_{V-A}\sum\nolimits_{q'}(\bar{q}'_\alpha q'_\beta)_{V-A},$$
$$Q_5=(\bar{q}_\alpha b_\alpha)_{V-A}\sum\nolimits_{q'}(\bar{q}'_\beta q'_\beta)_{V+A},$$
$$Q_6=(\bar{q}_\beta b_\alpha)_{V-A}\sum\nolimits_{q'}(\bar{q}'_\alpha q'_\beta)_{V+A}, \tag{9}$$

the electroweak penguins operator is expressed as follows:

$$Q_7=\frac{3}{2}(\bar{q}_\alpha b_\alpha)_{V-A}\sum\nolimits_{q'}e_{q'}(\bar{q}'_\beta q'_\beta)_{V+A},$$
$$Q_8=\frac{3}{2}(\bar{q}_\beta b_\alpha)_{V-A}\sum\nolimits_{q'}e_{q'}(\bar{q}'_\alpha q'_\beta)_{V+A},$$
$$Q_9=\frac{3}{2}(\bar{q}_\alpha b_\alpha)_{V-A}\sum\nolimits_{q'}e_{q'}(\bar{q}'_\beta q'_\beta)_{V-A},$$
$$Q_{10}=\frac{3}{2}(\bar{q}_\beta b_\alpha)_{V-A}\sum\nolimits_{q'}e_{q'}(\bar{q}'_\alpha q'_\beta)_{V-A}, \tag{10}$$

and the magnetic penguins operator is expressed as follows:

$$Q_{7\gamma}=\frac{e}{8\pi^2}m_b\bar{q}_\alpha\sigma^{\mu\nu}(1+\gamma_5)b_\alpha F_{\mu\nu},$$
$$Q_{8g}=\frac{g}{8\pi^2}m_b\bar{q}_\alpha\sigma^{\mu\nu}(1+\gamma_5)t^a_{\alpha\beta}b_\beta G^a_{\mu\nu}, \tag{11}$$

where $(\bar{q}_i q_j)_{V\pm A} \equiv \bar{q}_i \gamma_\mu (1 \pm \gamma_5) q_j$ and q' corresponds to a certain energy scale; we can take the flavor of all the free quarks at this energy scale. The weak decay of the B meson is $\mu \sim O(m_b)$ in the energy scale and $q' \in \{u, d, s, c, b\}$; $e_{q'}$ is the charge of the quark q'; α and β are color indices.

When dealing with the decay of the baryons into two mesons M_1 and M_2, the decay amplitudes are usually divided into emission and annihilation parts according to the topology structure. In the heavy quark limit, the emission part can be expressed as the product of the decay constant and form factor, while the weak annihilation part is generally considered to be suppressed by power. According to Eq. (7), the decay amplitudes of the B meson into the final state of the emission ($\mathcal{A}_E$) and weak annihilation ($\mathcal{A}_W$) parts have the following form [42]:

$$\mathcal{A}_E(B \to M_1 M_2) = \frac{G_F}{\sqrt{2}} \sum_{q=u,c} \sum_i V_q \alpha_i^q(\mu) \langle M_1 M_2 | Q_i | B \rangle_F , \tag{12}$$

$$\mathcal{A}_W(B \to M_1 M_2) = \frac{G_F}{\sqrt{2}} \sum_{q=u,c} \sum_i V_q f_B f_{M_1} f_{M_2} b_i(M_1, M_2), \tag{13}$$

where $\alpha_i^q(\mu)$ are flavour parameters that can be expressed in terms of the effective parameters α_i^q, which can be calculated perturbatively and has been demonstrated in a previous study [39]; f_B, f_{M_1}, and f_{M_2} are the decay constants associated with the initial and final mesons; the numerical results are usually extracted using experimental approaches.

In the heavy quark limit, ignoring the correction of Λ_{QCD}/m_b to the leading order, the effective operator of the hadron matrix element $\langle M_1 M_2 | Q_i | B \rangle$ can be calculated by the following formula using the QCDF:

$$\begin{aligned} &\langle M_1 M_2 | Q_i | B \rangle \\ &= \sum_j F_j^{B\to M_1} \int_0^1 \mathrm{d}x T_{ij}^I(x) \Phi_{M_2}(x) + (M_1 \leftrightarrow M_2) \\ &\quad + \int_0^1 \mathrm{d}\xi \int_0^1 \mathrm{d}x \int_0^1 \mathrm{d}y T_i^{II}(\xi, x, y) \Phi_B(\xi) \Phi_{M_1}(x) \Phi_{M_2}(y), \end{aligned} \tag{14}$$

where $F_j^{B\to M_1}$ represents the transition form factor of $B \to M_1$, T_{ij}^I and T_i^{II} are the computable hard scattering parts of the perturbation theory, and $\Phi_X(x)$ is the optical cone distribution amplitude of the quark—Fock state of the hadron, where the final hadrons M_1 and M_2 are both light mesons, or M_1 is a light meson and M_2 is a heavy quark even element. Then, when M_1 is a heavy meson and M_2 is a light meson, the hadron matrix element form is

$$\langle M_1 M_2 | Q_i | B \rangle = \sum_j F_j^{B\to M_1} \int_0^1 \mathrm{d}x T_{ij}^I(x) \Phi_{M_2}(x). \tag{15}$$

The calculation of hadron matrix elements in the two-body decay of the B meson becomes more straightforward using Eqs. (14) and (15). The non-perturbation effect is reflected in the amplitude and shape factor of the meson optical cone distribution. The form factor $F_j^{B\to M_1}$ is a physical quantity that contains both hard and soft contributions (therefore, the hard contribution needs to be subtracted from the hard scattering functions T_{ij}^I and T_i^{II}). This form factor can be determined from experiments on the semi-light decay of the B meson or from QCD theory. The light cone distribution amplitude of mesons can also be extracted from other hard scattering processes. The leading order of the decay amplitude corresponds to the contribution of naive factorization. In the heavy quark limit, the radiative corrections to the leading order can be calculated for all orders of α_s without considering the $1/m_b$ power correction.

Similarly, the weak annihilation contributions are described by the terms b_i and b_i^{EW}. They are expressed as

$$\begin{aligned} b_1(M_1, M_2) &= \frac{C_F}{N_c^2} C_1 A_1^i(M_1, M_2), \\ b_2(M_1, M_2) &= \frac{C_F}{N_c^2} C_2 A_1^i(M_1, M_2), \\ b_3(M_1, M_2) &= \frac{C_F}{N_c^2} \Big\{ C_3 A_1^i(M_1, M_2) + C_5 A_3^i(M_1, M_2) \\ &\quad + [C_5 + N_c C_6] A_3^f(M_1, M_2) \Big\}, \\ b_4(M_1, M_2) &= \frac{C_F}{N_c^2} \left\{ C_4 A_1^i(M_1, M_2) + C_6 A_2^i(M_1, M_2) \right\}, \\ b_3^{EW}(M_1, M_2) &= \frac{C_F}{N_c^2} \Big\{ C_9 A_1^i(M_1, M_2) + C_7 A_3^i(M_1, M_2) \\ &\quad + [C_7 + N_c C_8] A_3^f(M_1, M_2) \Big\}, \\ b_4^{EW}(M_1, M_2) &= \frac{C_F}{N_c^2} \left\{ C_{10} A_1^i(M_1, M_2) + C_8 A_2^i(M_1, M_2) \right\}, \end{aligned} \tag{16}$$

where the annihilation coefficients $b_{1,2}$ correspond to the current-current operator $Q_{1,2}$, the coefficients $b_{3,4}$ correspond to the QCD penguins operator $Q_{3\sim6}$, and the annihilation coefficients $b_{3,4}^{EW}$ correspond to the electroweak penguins operator $Q_{7\sim10}$. The amplitude $A_n^{i,f}(n = 1, 2, 3)$ comes from the annihilation contribution. The superscript i refers to gluon emission from the initial-state quark whereas the superscript f refers to gluon emission from the final-state quark. The form of $A_n^{i,f}$ was confirmed in Ref. [39]. Besides, we managed the endpoint integrals of these logarithmic divergences arising from the hard scattering process involving the spectator quark. We extended phenomenological parameters to express it in the

form of $X \equiv \int_0^1 dx/x = (1+\rho_A e^{i\phi_A})(\ln m_B/\Lambda_h)$, which is calculated according to the method described in Refs. [12, 43, 44], where one may assume $\rho_A \leq 0.5$ and arbitrary strong phases ϕ_A. In practice, we calculated the CP asymmetry for $\rho_A = 0.25, 0.5$ and $\phi_A = 0, \pi/2, \pi, 3\pi/2$, respectively. The value of Λ_h was set to 0.5 GeV. Regarding the values of the parameters ϕ_A and ρ_A, we followed the latest achievements and applied the latest constraints, assigning an uncertainty of ±0.1 to ϕ_A and ±20° to ρ_A. QCDF has been shown to be effective in the calculations of the non-light and weak decays of the B meson, including chirally enhanced corrections.

C. Amplitude of $\bar{B}_s^0 \to \pi^+\pi^- P$ involving $\rho-\omega-\phi$ interference

Under the framework of QCDF, we analyzed the resonance effect generated by mixing intermediate particles for CP asymmetry and branching ratio of $\bar{B}_s^0$. The decay processes $\bar{B}_s^0 \to \pi^+\pi^- P$ involving $\rho(\omega,\phi)$ mesons are shown in Fig. 1, where P represents the final pseudo-scalar meson. Considering the $\rho \to \pi^+\pi^-$ process from isospin symmetry breaking, we conclude that the vector meson to $\pi^+\pi^-$ can be attributed to the existence of $\omega-\rho$ and $\phi-\rho$ meson intermediate states of resonance effect. Therefore, we only considered the decay process of the key intermediate state particle $\rho \to \pi^+\pi^-$ and dismissed the $\rho^- \to \pi^-\pi^0$ and $\rho^+ \to \pi^+\pi^0$ decay processes in our approach. The influence of the resonance effect on CP asymmetry, considering the interference of intermediate particles, is shown in panels (b), (c), (e), (f), (h), and (i) of Fig. 1. Taking Fig. 1(b) as an example, $\bar{B}_s^0$ decays into ω mesons and pseudo-scalar meson P, ω can decay into ρ mesons first and then these ρ mesons decay into $\pi^+\pi^-$ mesons. In this process, the resonance effect generated by the interaction between ω and ρ mesons is involved, and the CP asymmetry and branching ratio in the resonance state can be calculated.

To the first leading order in isospin breaking, the main contributions come from panels (b) and (c) in Fig. 1. Therefore, the CP asymmetry results shown in panels (a), (b), and (c) were further calculated. The CP asymmetry results are significantly suppressed in the other processes where the decay rate is relatively low under the resonance effect, so we did not consider them.

We employed a quasi-two-body decay process to calculate the CP asymmetry and branching ratio. In the two-body decay of the B meson, the form factor governing the transition from the initial to the final hadrons is dominated by non-perturbative effects [45]. We can calculate the perturbative contribution associated with the hard gluon from the QCD correction. In the three-body decay process, we adopted the naive Breit-Wigner form for ρ with pole mass m_ρ = 0.775 GeV and width ρ = 0.149 GeV [46]. For example, the decay process of $\bar{B}_s^0 \to \rho(\rho \to \pi^+\pi^-)\pi^0$ can be expressed as

$$\mathcal{M}_\rho = \frac{\langle \rho\pi^0 | \mathcal{H}_{\rm eff} | \bar{B}_s^0 \rangle \langle \pi^+\pi^- | \mathcal{H}_{\rho\pi^+\pi^-} | \rho \rangle}{s - m_\rho^2 + i m_\rho \Gamma_\rho}, \tag{17}$$

where $\mathcal{H}_{\rho\pi^+\pi^-}$ denotes the effective Hamiltonians of the strong processes $\rho \to \pi^+\pi^-$, $s - m_\rho^2 + i m_\rho \Gamma_\rho$ is the Breit-Wigner form for the propagator of ρ, and s is the invariant mass squared of mesons π^+ and π^-.

Next, we present the decay amplitude for the quasi-

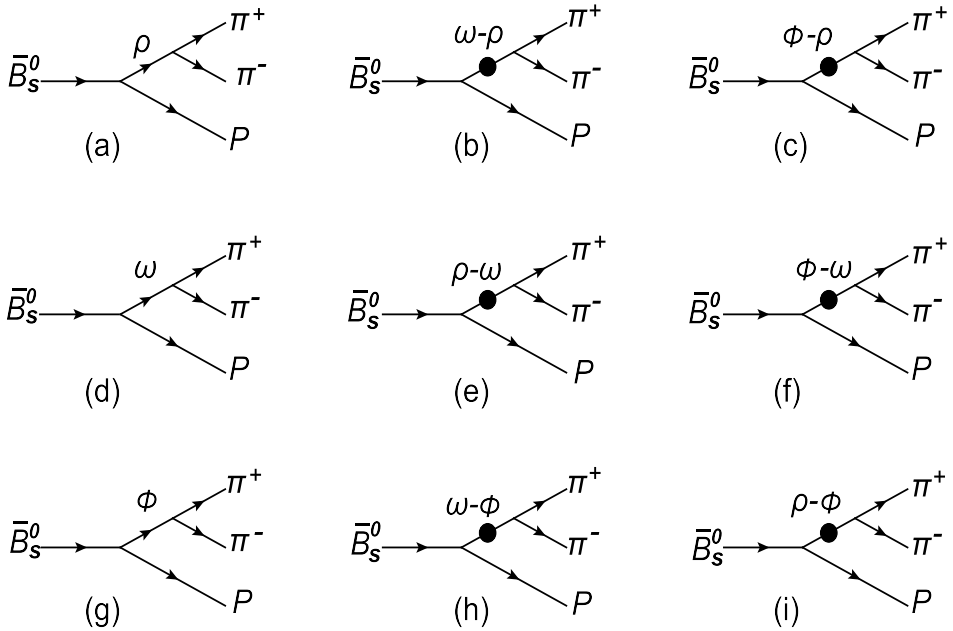

Fig. 1. Decay processes for the channel of $\bar{B}_s^0 \to \rho(\omega,\phi)P \to \pi^+\pi^- P$.

two-body decay, including both emission and annihilation contributions, for $\bar{B}_s^0 \to \rho(\rho \to \pi^+\pi^-)\pi^0$ under QCDF. The remaining amplitude forms of $B \to VP \to \pi^+\pi^- P$ are provided in Appendix A.

$$\mathcal{M}\left(\bar{B}_s^0 \to \rho(\rho \to \pi^+\pi^-)\pi^0\right) = \sum_{q=u,c} \frac{G_F g_{\rho\pi^+\pi^-} f_{B_s} f_\pi f_\rho}{2\sqrt{2}s_\rho} \left\{ V_{ub}V_{us}^*[b_1(\pi,\rho)+b_1(\rho,\pi)] - V_{tb}V_{ts}^* \left[2b_4(\pi,\rho) + 2b_4(\rho,\pi) + \frac{1}{2}b_4^{EW}(\pi,\rho) + \frac{1}{2}b_4^{EW}(\rho,\pi) \right] \right\}, \tag{18}$$

$$\mathcal{M}\left(\bar{B}_s^0 \to \omega(\omega \to \pi^+\pi^-)\pi^0\right) = \sum_{q=u,c} \frac{G_F g_{\omega\pi^+\pi^-} f_{B_s} f_\pi f_\omega}{2\sqrt{2}s_\omega} \left\{ V_{ub}V_{us}^*[b_1(\pi,\omega)+b_1(\omega,\pi)] - V_{tb}V_{ts}^* \left[\frac{3}{2}b_4^{EW}(\pi,\omega) + \frac{3}{2}b_4^{EW}(\omega,\pi) \right] \right\}, \tag{19}$$

$$\mathcal{M}\left(\bar{B}_s^0 \to \phi(\phi \to \pi^+\pi^-)\pi^0\right) = \sum_{q=u,c} \frac{G_F g_{\phi\pi^+\pi^-} m_\phi \epsilon(\lambda)\cdot p_\pi}{s_\phi} \left\{ V_{ub}V_{us}^* f_\pi A_0^{B_s^0\to\phi} a_2 + V_{tb}V_{ts}^* \left[f_\pi A_0^{B_s^0\to\phi} \left(\frac{3}{2}a_7 - \frac{3}{2}a_9 \right) \right] \right\}, \tag{20}$$

where $V_{ub}V_{us}^*$ and $V_{tb}V_{ts}^*$ are CKM matrix elements, and s_ρ, s_ω, and s_ϕ are the Breit-Wigner factors. The decay constants f_π, f_{B_s}, and $f_{\rho(\omega,\phi)}$ correspond to non-perturbative contributions, while the coefficients $a_{1,2\ldots n}$ are associated with the Wilson coefficient C_i [47]. The form factors for the process $B \to \phi$ are denoted by $A_0^{B_s^0\to\phi}$, which arise from non-perturbative effects. Additionally, annihilation contributions given by b_1, b_4, and b_4^{EW} were considered in Ref. [48]. Interestingly, the contribution of the $\bar{B}_s^0 \to \rho(\omega)\pi^0 \to \pi^+\pi^-\pi^0$ decay process is dominated by the annihilation contribution, while there is no annihilation contribution in the amplitude of the $\bar{B}_s^0 \to \phi\pi^0 \to \pi^+\pi^-\pi^0$ decay process. Here, ϵ denotes the polarization vector meson, p_π represents the momentum of π, and $g_{V\pi^+\pi^-}$ denotes the effective coupling constants, which can be expressed in terms of the decay width of $V \to \pi^+\pi^-$. At this point, the hard scattering part of the QCDF depends only on s, while the non-perturbative part remains in the same form as that of the two-body decay. Furthermore, we define a mass parameter that characterizes the quark mass related to the meson component in O_i. The values of some input parameters and constants are provided in Appendix B [24, 49].

III. CP ASYMMETRY AND BRANCHING RATIO

A. Form of strong phase of CP asymmetry

The total amplitude used in the calculations is denoted by $\mathcal{M}$, where $\mathcal{M}$ represents the sum of the tree ($\langle\pi^+\pi^- P|H^T|\bar{B}_s^0\rangle$) and penguin ($\langle\pi^+\pi^- P|H^P|\bar{B}_s^0\rangle$) contributions. The relative strong phase angle δ and weak phase angle ϕ affect CP asymmetry, where the strong phase angle δ arises from the resonance effect and the weak phase angle ϕ originates from the CKM matrix. We then define the new total amplitude as the ratio of the penguin to the tree contributions [29]:

$$\mathcal{M} = \langle\pi^+\pi^- P|H^T|\bar{B}_s^0\rangle[1 + re^{i(\delta+\phi)}], \tag{21}$$

where the parameter r represents the ratio between the amplitude contributions of the penguin and tree levels. Furthermore, considering the interference of $\omega-\rho$ and $\phi-\rho$, we can derive a detailed form of the tree and penguin amplitudes by combining the decay diagrams in Fig. 1:

$$\begin{aligned}\langle\pi^+\pi^- P|H^T|\bar{B}_s^0\rangle = {} & \frac{g_{\rho\to\pi^+\pi^-}T_\rho}{s-m_\rho^2+im_\rho\Gamma_\rho} \\ & + \frac{g_{\rho\to\pi^+\pi^-}\widetilde{\Pi}_{\rho\omega}T_\omega}{(s-m_\rho^2+im_\rho\Gamma_\rho)(s-m_\omega^2+im_\omega\Gamma_\omega)} \\ & + \frac{g_{\rho\to\pi^+\pi^-}\widetilde{\Pi}_{\rho\phi}T_\phi}{(s-m_\rho^2+im_\rho\Gamma_\rho)(s-m_\phi^2+im_\phi\Gamma_\phi)},\end{aligned} \tag{22}$$

$$\begin{aligned}\langle\pi^+\pi^- P|H^P|\bar{B}_s^0\rangle = {} & \frac{g_{\rho\to\pi^+\pi^-}P_\rho}{s-m_\rho^2+im_\rho\Gamma_\rho} \\ & + \frac{g_{\rho\to\pi^+\pi^-}\widetilde{\Pi}_{\rho\omega}P_\omega}{(s-m_\rho^2+im_\rho\Gamma_\rho)(s-m_\omega^2+im_\omega\Gamma_\omega)} \\ & + \frac{g_{\rho\to\pi^+\pi^-}\widetilde{\Pi}_{\rho\phi}P_\phi}{(s-m_\rho^2+im_\rho\Gamma_\rho)(s-m_\phi^2+im_\phi\Gamma_\phi)},\end{aligned} \tag{23}$$

where $T_{\rho(\omega,\phi)}$ and $P_{\rho(\omega,\phi)}$ are the tree and penguin contributions for the $\bar{B}_s^0 \to \rho(\omega,\phi)P$ decay process, respectively. In this study, the tree contribution is associated with $V_{ub}V_{us}^*$

whereas the penguin contribution is associated with $V_{tb}V_{ts}^*$ in Eqs. (18)−(20) and Appendix A; s is the invariant mass squared of mesons $\pi^+\pi^-$ [50]. By using the tree and penguin contributions, we derived new strong phases. These phases include $P_\omega/T_\rho \equiv r_1 e^{i(\delta_\lambda+\phi)}$, $P_\phi/T_\rho \equiv r_2 e^{i(\delta_x+\phi)}$, $T_\omega/T_\rho \equiv r_3 e^{i\delta_\alpha}$, $T_\phi/T_\rho \equiv r_4 e^{i\delta_\tau}$, and $P_\rho/P_\omega \equiv r_5 e^{i\delta_\beta}$. Here δ_λ, δ_x, δ_α, δ_τ, and δ_β represent strong phases. The results can be substituted into Eq. (21). After simplification, we obtain

$$re^{i\delta} = \frac{r_1 e^{i\delta_\lambda} r_5 e^{i\delta_\beta} s_\phi s_\omega + r_2 e^{i\delta_x} s_\omega \widetilde{\Pi}_{\rho\phi} + r_1 e^{i\delta_\lambda} s_\phi \widetilde{\Pi}_{\rho\omega}}{r_4 e^{i\delta_\tau} s_\omega \widetilde{\Pi}_{\rho\phi} + s_\phi s_\omega + r_3 e^{i\delta_\alpha} s_\phi \widetilde{\Pi}_{\rho\omega}}. \tag{24}$$

The weak phase ϕ is determined by the ratio of $V_{ub}V_{ud}^*$ to $V_{tb}V_{td}^*$ or the ratio of $V_{ub}V_{us}^*$ to $V_{tb}V_{ts}^*$ in the CKM matrix. We conclude that $\sin\phi = \eta/\sqrt{(\rho-\rho^2-\eta^2)^2+\eta^2}$ and $\cos\phi = (\rho-\rho^2-\eta^2)/\sqrt{(\rho-\rho^2-\eta^2)^2+\eta^2}$, or $\sin\phi = -\eta/\sqrt{\rho^2+\eta^2}$ and $\cos\phi = -\rho/\sqrt{\rho^2+\eta^2}$ according to the Wolfenstein parameters [34].

B. Local integral form of CP asymmetry

We provide a reference for future experiments by integrating A_{CP} over the phase space in this subsection. The amplitude for the decay process of $\bar{B}_s^0 \to \rho\pi^0$ can be given by $M^\lambda_{\bar{B}_s^0\to\rho\pi^0} = \alpha p_{\bar{B}_s^0}\cdot\epsilon^*(\lambda)$, where λ is the direction of polarization for ϵ; ϵ is the ρ mean polarization vector; $p_{\bar{B}_s^0}$ is the $\bar{B}_s^0$ momentum of the meson; and α represents the part of the amplitude which is independent of λ. The decay process $\rho\to\pi^+\pi^-$ can be described as $M^\lambda_{\rho\to\pi^+\pi^-} = g_\rho\epsilon(\lambda)(p_1-p_2)$, where p_1 and p_2 denote the momenta of π^+ and π^- generated by the ρ meson [44, 51]. Therefore, the total amplitude of the $\bar{B}_s^0\to\rho\pi^0\to\pi^+\pi^-\pi^0$ decay process can be expressed as

$$A = \alpha p^\mu_{\bar{B}_s^0}\frac{\sum_\lambda \epsilon^*_\mu(\lambda)\epsilon_\nu(\lambda)}{s_\rho}\frac{g_\rho}{s_\rho}(p_1-p_2)^\nu, \tag{25}$$

where $\sqrt{s}$ and $\sqrt{s'}$ represent the low and high invariant masses of the $\pi^+\pi^-$ pair, and $s'_{\max}$ and $s'_{\min}$ are the maximum and minimum values of s' for a fixed s, respectively [52]. We obtained $m_{ij}^2 = p_{ij}^2$ by applying conservation of momentum and energy during the three-body decay process. Therefore, the amplitude can be expressed as

$$A = \frac{g_\rho}{s_\rho}\cdot\frac{M^\lambda_{\bar{B}_s^0\to\rho\pi^0}}{p_{\bar{B}_s^0}\cdot\epsilon^*}\cdot(\sigma-s') = (\sigma-s')\cdot\mathcal{M}, \tag{26}$$

where $\mathcal{M}$ is the substitution of the previous formula and σ is assumed to be a constant related to s, where $\sigma = \frac{1}{2}\left(s'_{\max}+s'_{\min}\right)$. For a fixed s, the differential CP asymmetry parameter can be defined as $A_{\rm CP} = (|\mathcal{M}|^2 - |\overline{\mathcal{M}}|^2)/(|\mathcal{M}|^2+|\overline{\mathcal{M}}|^2)$. Subsequently, we integrate the denominator and numerator of $A_{\rm CP}$ within the range of $\Omega\left(s_1<s<s_2, s'_1<s'<s'_2\right)$. The resulting localized integrated CP asymmetry is [53]

$$A^\Omega_{CP} = \frac{\int_{s_1}^{s_2}{\rm d}s\int_{s'_1}^{s'_2}{\rm d}s'(\sigma-s')^2\left(|\mathcal{M}|^2-|\overline{\mathcal{M}}|^2\right)}{\int_{s_1}^{s_2}{\rm d}s\int_{s'_1}^{s'_2}{\rm d}s'(\sigma-s')^2\left(|\mathcal{M}|^2+|\overline{\mathcal{M}}|^2\right)}. \tag{27}$$

Given that s varies in a small region, σ can be approximately treated as a constant. Thus, we can cancel the influence of $\int_{s'_1}^{s'_2}{\rm d}s'(\sigma-s')^2$ [54]. It is assumed that $s'_{\min} < s' < s'_{\max}$ represents an integral interval of the high invariance mass of $\pi^+\pi^-$, while $\int_{s'_{\min}}^{s'_{\max}}{\rm d}s'(\sigma-s')^2$ represents a factor that depends on s.

C. Decay branching ratio under resonance effect

Owing to isospin breaking, the effects of three-particle mixing on the branching ratios of $\bar{B}_s^0\to\rho(\omega,\phi)\pi^0(\bar{K}^0,\eta,\eta')\to\pi^+\pi^-\pi^0(\bar{K}^0,\eta,\eta')$ are symmetrical. By considering the value of $g_{\rho\to\pi^+\pi^-}$ [28], we calculate the branching ratios of $\bar{B}_s^0\to\pi^+\pi^-\pi^0(\bar{K}^0,\eta,\eta')$ under the three-particle mixing. The formula for the differential branching ratios originates from the S-wave contribution reported by Particle Data Group (PDG) [24]. However, we consider the process that primarily involves the P-wave contribution [55]. The differential branching ratios for the quasi-two-body $\bar{B}_s^0\to VP\to\pi^+\pi^-P$ decays are expressed as [55−57]

$$\frac{{\rm d}B}{{\rm d}\xi} = \frac{\tau_{B_s}q_A^3 q^3}{48\pi^3 m_{B_s}^5}|\bar{\mathcal{A}}|^2, \tag{28}$$

with the variable given by $\xi = s/m_{B_s}^2$ and the B meson mean lifetime denoted as τ_B. Here, q is already explained in Eq. (3) and q_A is defined as [28]:

$$q_A = \frac{1}{2}\sqrt{\left[\left(m_{B_s}^2-m_P^2\right)^2 - 2\left(m_{B_s}^2+m_P^2\right)s+s^2\right]/s}, \tag{29}$$

where m_P is the mass of the pseudoscalar meson obtained from the momentum analysis of the final-state particle.

IV. NUMERICAL RESULTS

A. Curve results of localized CP asymmetry

We calculated the decay amplitudes for the quasi-two-body decay process in the framework of QCDF using Eqs. (18) to (20). One can see that the decay amplitudes depend on CKM matrix elements, decay constants, form factors, and Wilson coefficients for each final state particle. The strong phase δ and absolute value r of the ratio of the penguin to tree amplitudes can be calculated using the QCDF approach and vary for different

final state particles. Given the previous results, we set the same threshold range for the resonance effect of vector meson mixing [6]. The Particle Data Group (PDG) data show that the masses of ρ, ω, and ϕ are estimated to be 0.775, 0.782, and 1.019 GeV, respectively [24]. We selected the region $0.65-1.10$ GeV within our theoretical framework, where the resonance effects of mixing $\omega-\rho$ and $\phi-\rho$ can be visually observed. This is the main resonance region, with the decay process $V(\rho,\omega,\phi)\to\pi^+\pi^-$, used to plot A_{CP} as a function of $\sqrt{s}$. The change in CP asymmetry for each decay process under the influence of the resonance effect is represented in Figs. 2–5. Moreover, the invariant mass of $\pi^+\pi^-$ is shown around the mass of $\rho(\omega,\phi)$ meson. Therefore, the overall CP asymmetry is observed for numbers ranging from 0.65 to 1.10 GeV [6]. The results are shown in Figs. 2 and 3, which illustrate the interrelation between CP asymmetry and $\sqrt{s}$. Note the significant peak in the CP asymmetry for the four decay modes of $\bar{B}_s^0\to\rho(\omega,\phi)\pi^0(\bar{K}^0,\eta,\eta')\to\pi^+\pi^-\pi^0(\bar{K}^0,\eta,\eta')$ owing to the ρ, $\omega-\rho$, and $\phi-\rho$ resonances in Figs. 2, 3, 4 , and 5 , where ρ dominates.

Given that $\bar{B}_s^0\to\rho\pi^0$ and $\bar{B}_s^0\to\omega\pi^0$ have no tree level contribution for the $\bar{B}_s^0\to\pi^+\pi^-\pi^0$ decay mode, the generation of CP asymmetry is mainly due to the weak annihilation contribution. Its CP asymmetries, ranging from 24.51% to –3.30%, are observed in the resonance regions of $\omega-\rho$, and significant CP asymmetries ranging from 0.39% to –1.72% are observed in the resonance regions of $\phi-\rho$, as shown in Fig. 2. For the $\bar{B}_s^0\to\pi^+\pi^-\bar{K}^0$ decay process, large CP asymmetries ranging from 97.41% to –36.51% are observed in the resonance regions of $\omega-\rho$. In the resonance regions of $\phi-\rho$, CP asymmetries ranging from 7.81% to 2.15% are observed, as depicted in Fig. 3. Thus, there is a large change in the CP asymmetry between the resonance regions of $\omega-\rho$ for $\bar{B}_s^0\to\pi^+\pi^-\bar{K}^0$ and $\bar{B}_s^0\to\pi^+\pi^-\pi^0$; the CP asymmetry varies slightly around the $\phi-\rho$ resonance range under QCDF.

In addition, we calculated the decay process $\bar{B}_s^0\to V\eta(\eta')\to\pi^+\pi^-\eta(\eta')$. In the $SU(3)$ quark representation of hadrons, the corresponding parameters are more difficult to determine owing to the octet-singlet mixing. The Feldmann-KrollStech (FKS) mixing scheme was adopted in this study for $\eta-\eta'$ mixing [58]. The parameters in the calculations can be expressed by f_q, f_s, and ϕ; specific amplitude forms are provided in Appendix A. The physical states of the η and η' mesons consist of a mixture of flavor eigenstates, namely η_n and η_s. We observe CP asymmetries ranging from 0.47% to –12.79% within the resonance range of $\omega-\rho$ in the decay channel of $\bar{B}_s^0\to\pi^+\pi^-\eta$ and CP asymmetries ranging from 5.77% to 0.25% within the resonance range of $\phi-\rho$ in Fig. 4. In the case of $\bar{B}_s^0\to\pi^+\pi^-\eta'$, we found significant CP asymmetries

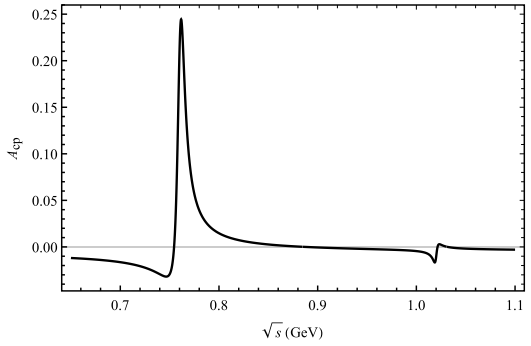

Fig. 2. Curve corresponding to the decay channel of $\bar{B}_s^0\to\pi^+\pi^-\pi^0$.

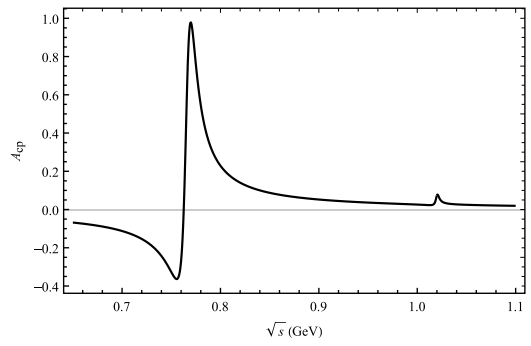

Fig. 3. Curve corresponding to the decay channel of $\bar{B}_s^0\to\pi^+\pi^-\bar{K}^0$.

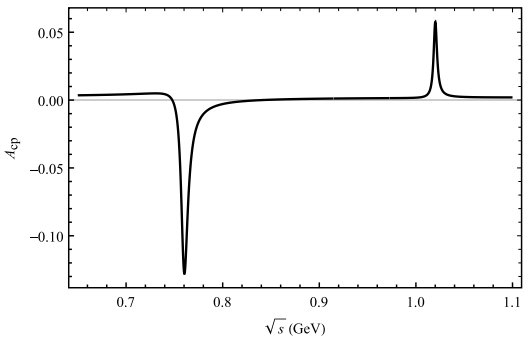

Fig. 4. Curve corresponding to the decay channel of $\bar{B}_s^0\to\pi^+\pi^-\eta$.

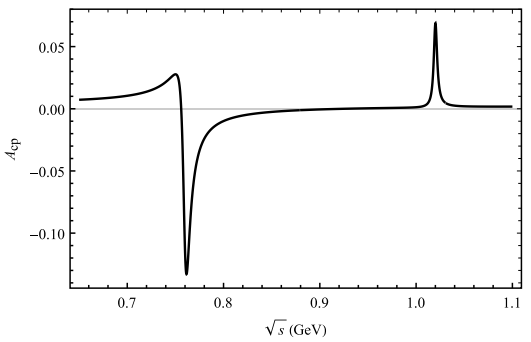

Fig. 5. Curve corresponding to the decay channel of $\bar{B}_s^0\to\pi^+\pi^-\eta'$.

ranging from 2.76% to −13.29% within the $\omega-\rho$ resonance region, and CP asymmetries ranging from 6.85% to 0.14% within the $\phi-\rho$ resonance region, as depicted in Fig. 5. The CP asymmetry in the decay process $\bar{B}_s^0 \to \pi^+\pi^-\eta'$ exhibits a significant variation similar to that observed in the decay process of $\bar{B}_s^0 \to \pi^+\pi^-\eta$, specifically within the mass resonances of $\omega-\rho$. Similarly, the CP asymmetry of these two decay processes also varies in the $\phi-\rho$ resonance region.

These results were obtained using the central parameter values of the CKM matrix elements. The CP asymmetry results observed in these decays will hopefully provide valuable insights for analyzing fundamental physical phenomena involving the interference of vector mesons.

B. Local integral CP asymmetry

Given that there are no experimentally measured results for $\rho-\omega-\phi$ mixing, we calculated the integral result of the CP asymmetry for $\bar{B}_s^0 \to \rho(\omega,\phi)\pi^0(\bar{K}^0) \to \pi^+\pi^-\pi^0(\bar{K}^0)$ to compare with the result from PQCD presented in this paper. We also calculated the $\bar{B}_s^0 \to \rho(\omega,\phi)\eta(\eta') \to \pi^+\pi^-\eta(\eta')$ decay processes by integrating over the invariant masses of $m_{\pi^+\pi^-}$ in the range of 0.65−1.1 GeV from the ρ, ω, and ϕ resonance regions [46]. In addition, we calculated the region between 0.75 and 0.82 GeV, where the CP asymmetry is clearly exhibited, as shown in Figs. 2−5. The results are provided in Table 1.

Subsequently, we compared the previous PQCD results to analyze the differences between the same decay processes. It is worth noting that the decay of $\bar{B}_s^0 \to \pi^+\pi^-\bar{K}^0$ with resonance effect has a significant effect on the CP asymmetry in the same energy range under QCDF. The CP asymmetry result of decay $\bar{B}_s^0 \to \pi^+\pi^-\pi^0$ is significantly smaller than that of the previous PQCD approach, possibly because the amplitude contribution of the quasi-two-body decay of $\bar{B}_s^0 \to \pi^+\pi^-\pi^0$ is primarily composed of the penguin and annihilation contributions. Besides, we added the two decay processes, namely $\bar{B}_s^0 \to \rho(\omega,\phi)\eta \to \pi^+\pi^-\eta$ and $\bar{B}_s^0 \to \rho(\omega,\phi)\eta' \to \pi^+\pi^-\eta'$, and calculated the CP asymmetry result affected by the resonance effect. The local CP asymmetry results for all decay processes are clearly enhanced within the 0.75 − 0.82 GeV region under the invariant mass region of $\omega-\rho$ mesons, especially for the decay processes of $\bar{B}_s^0 \to \pi^+\pi^-\pi^0$ and $\bar{B}_s^0 \to \pi^+\pi^-\eta'$. The CP asymmetry result of $\bar{B}_s^0 \to \pi^+\pi^-\eta$ is smaller than the result produced by other decay processes within the region of 0.75−0.82 GeV, which corresponds to the mass resonances of $\omega-\rho$.

There are two sources of uncertainty in our numerical results: the first arises from the uncertainty of the mixing parameter and other input parameters, and the second is due to the parameterization of the logarithmically divergent integral in QCDF.

C. Decay branching ratio

In view of the specific experimental data results of the decay branch ratio of the quasi two-body decay $\bar{B}_s^0 \to \rho(\omega,\phi)P \to \pi^+\pi^-P$ process without the resonance effect, we only refer to the theoretical results of the latest relevant studies. The branching ratio of the three-body decay of B_s mesons has been studied more extensively using the PQCD approach, but the calculation results of the branching ratio under the $\rho-\omega-\phi$ mixing mechanism have not been considered. Therefore, we only used the results of the direct decay of $\bar{B}_s^0 \to \rho P \to \pi^+\pi^-P$ for comparison. Given that the FAT approach includes power corrections from the "chirally enhanced" term, the penguin annihilation contribution, and the EW-penguin diagram for the $\bar{B}_s^0 \to VP$ decay process, and some of their results closely match experimental results, we used them for comparison.

When we calculated the branching ratio under the $\rho-\omega-\phi$ resonance effect, we observed that the branching ratio of the decay of $\bar{B}_s^0 \to \rho P \to \pi^+\pi^-P$ is not affected by resonance effects. The calculation results of the branch ratio of quasi-two-body decay based on $\rho-\omega-\phi \to \pi^+\pi^-$ are listed in Table 2 for easy comparison and analysis.

By comparison, it can be seen that in the direct decay process of $\bar{B}_s^0 \to \rho P \to \pi^+\pi^-P$, the decay branching ratio calculated by the three approaches is of one order of magnitude. For the $\bar{B}_s^0 \to \pi^+\pi^-\pi^0$ process, the result obtained from the QCDF approach is lower than that of the other two processes because the decay amplitude of the process is dominated by the annihilation graph. For the decay process of $\bar{B}_s^0 \to \pi^+\pi^-\bar{K}^0$, the results of the QCDF approach are close to those of the PQCD approach, but the details of the FAT approach are finer, which may be caused by the shortage of non perturbative contribution

Table 1. Comparison of A_{cp}^{Ω} from $\rho-\omega-\phi$ mixing with $V \to \pi^+\pi^-$.

Decay channel	$\rho-\omega-\phi$ mixing (PQCD) (0.65−1.1 GeV) [6, 24]	$\rho-\omega-\phi$ mixing (QCDF) (0.65−1.1 GeV)	$\rho-\omega-\phi$ mixing (QCDF) (0.75−0.82 GeV)
$\bar{B}_s^0 \to \rho(\omega,\phi)\pi^0 \to \pi^+\pi^-\pi^0$	-0.008 ± 0.002	$-0.001 \pm 0.003 \pm 0.007$	$0.014 \pm 0.006 \pm 0.011$
$\bar{B}_s^0 \to \rho(\omega,\phi)\bar{K}^0 \to \pi^+\pi^-\bar{K}^0$	-0.017 ± 0.003	$0.053 \pm 0.014 \pm 0.006$	$0.31 \pm 0.015 \pm 0.020$
$\bar{B}_s^0 \to \rho(\omega,\phi)\eta \to \pi^+\pi^-\eta$	–	$0.001 \pm 0.006 \pm 0.001$	$-0.003 \pm 0.003 \pm 0.008$
$\bar{B}_s^0 \to \rho(\omega,\phi)\eta' \to \pi^+\pi^-\eta'$	–	$0.001 \pm 0.002 \pm 0.004$	$-0.009 \pm 0.008 \pm 0.006$

Table 2. Branching ratio ($\times 10^{-6}$) of $\bar{B}_s^0 \to VP \to \pi^+\pi^- P$.

Decay channel	PQCD approach [24, 59] $\rho \to \pi^+\pi^-$	FAT approach [24, 28] $\rho \to \pi^+\pi^-$	QCDF approach $\rho \to \pi^+\pi^-$ $\rho-\omega-\phi \to \pi^+\pi^-$
$\bar{B}_s^0 \to \pi^+\pi^-\pi^0$	$0.35\ ^{+0.06}_{-0.05} \pm 0.01 \pm 0.00$	$0.35 \pm 0.05 \pm 0.01 \pm 0.03$	$0.16 \pm 0.03 \pm 0.02 \pm 0.04$ $0.15 \pm 0.04 \pm 0.09 \pm 0.01$
$\bar{B}_s^0 \to \pi^+\pi^-\bar{K}^0$	$0.21\ ^{+0.05}_{-0.01}\ ^{+0.01}_{-0.00}\ ^{+0.01}_{-0.00}$	$1.55 \pm 1.10 \pm 0.31 \pm 0.02$	$0.12 \pm 0.05 \pm 0.09 \pm 0.04$ $0.08 \pm 0.06 \pm 0.02 \pm 0.00$
$\bar{B}_s^0 \to \pi^+\pi^-\eta$	$0.10\ ^{+0.04}_{-0.02} \pm 0.00 \pm 0.00$	$0.11 \pm 0.02 \pm 0.02 \pm 0.03$	$0.32 \pm 0.04 \pm 0.03 \pm 0.03$ $0.30 \pm 0.01 \pm 0.04 \pm 0.05$
$\bar{B}_s^0 \to \pi^+\pi^-\eta'$	$0.23\ ^{+0.08}_{-0.06}\ ^{+0.00}_{-0.01} \pm 0.00$	$0.34 \pm 0.07 \pm 0.05 \pm 0.01$	$0.22 \pm 0.04 \pm 0.05 \pm 0.02$ $0.20 \pm 0.06 \pm 0.03 \pm 0.01$

and $1/m_b$ power corrections of the FAT approach. As a result of the direct decay process of $\bar{B}_s^0 \to \pi^+\pi^-\eta$, the QCDF result is larger than that of the other two processes, which may be due to the uncertainty introduced by the form factor itself of the QCDF approach. In the decay process of $\bar{B}_s^0 \to \pi^+\pi^-\eta'$, the results obtained from QCDF and PQCD are consistent, and the differences between the QCDF results and those from the FAT approach are extremely small. Owing to the difference in the treatment of intermediate virtual particles in the FAT approach, these results may be biased.

Above all, we calculated the decay branching ratio of these four decay processes under the $\rho-\omega-\phi$ resonance effect. We found that the results of each decay branching ratio are suppressed, especially for the $\bar{B}_s^0 \to \pi^+\pi^-\bar{K}^0$ decay process. We hypothesize that the mixing of the intermediate state meson $\rho-\omega-\phi$ suppresses the decay branching ratio. Given that intermediate virtual particles such as $\rho-\omega$ cannot be effectively distinguished experimentally, it is necessary to consider the effects of mixing of intermediate virtual particles in future research.

Similarly, different sources of uncertainty were also considered in the calculations. The first source arises from the CKM matrix elements, form factors, and decay constants; the second source comes from the QCDF approach itself during the calculation process; and the third source is due to the mixing parameters.

V. CONCLUSIONS

Our results show that CP asymmetries and decay branching ratios undergo evident changes due to the resonance effect of $V \to \pi^+\pi^-$ $(V = \rho, \omega, \phi)$ in the $B \to \pi^+\pi^- P$ decay modes when the invariant mass of $\pi^+\pi^-$ is close to the $\omega-\rho$ and $\phi-\rho$ resonance regions within the QCDF framework.

The three-body decay process was efficiently calculated using the quasi-two-body chain decay. Taking $B \to RP_3$ as an example, the intermediate resonance state R decays into two hadrons, P_1 and P_2, while P_3 is the other hadron. This process can be decomposed using the narrow width approximation as $\mathcal{B}(B \to RP_3 \to P_1P_2P_3) = \mathcal{B}(B \to RP_3)\mathcal{B}(B \to P_1P_2)$. In small widths, the effects of ω and ϕ can be ignored in the quasi-two-body cascade decay. As a measure of the degree of approximation of $\Gamma(B \to RP_3)\mathcal{B}(B \to P_1P_2) = \eta_R\Gamma(B \to RP_3 \to P_1P_2P_3)$, the parameter η_R was introduced [60]. The integral of the invariant mass $m_{\pi^+\pi^-}$ was considered in the calculations. The attenuation amplitude features a Breit-Wigner shape and depends on the parameter of the invariant mass $m_{\pi^+\pi^-}$. In the present study, the effect of this correction was ignored in view of the range of accuracy. This level of correction was approximately 7%, being a source of uncertainty in our results [46].

Regarding the local integration results (Table 1), the local CP asymmetry associated with $B \to \rho(\omega,\phi)P \to \pi^+\pi^-P$was determined by calculating the specific phase space region. Owing to the interference of $\rho-\omega-\phi$ caused by the breaking of isospin, the resonance contribution of $\omega-\rho$ and $\phi-\rho$ can produce a new strong phase, which has a great influence on the CP asymmetry of the $B \to \pi^+\pi^-P$ decay mode. It is evident that for the $\bar{B}_s^0 \to \pi^+\pi^-\pi^0$ process, the result obtained from the QCDF approach is significantly smaller than that obtained from the PQCD approach. This is because the amplitude contribution of the $\bar{B}_s^0 \to \pi^+\pi^-\pi^0$ process is dominated by the penguin and annihilation contributions. On the contrary, the CP asymmetry result of the $\bar{B}_s^0 \to \pi^+\pi^-\bar{K}^0$ process is considerably larger owing to the evident tree and penguin level contributions in this process, while the uncertainty of the form factor and decay constant further adds to the overall uncertainty of the results. For the newly added decay processes of $\bar{B}_s^0 \to \pi^+\pi^-\eta$ and $\bar{B}_s^0 \to \pi^+\pi^-\eta'$, when the threshold interval was in the range 0.75−0.82 GeV, the local integral result became significantly larger, indicating that the CP asymmetry of $\bar{B}_s^0 \to \pi^+\pi^-\eta$ and $\bar{B}_s^0 \to \pi^+\pi^-\eta'$ decays primarily occurs in the mixing region of $\omega-\rho$ given that ρ is dominant.

In the process of calculating the decay branching ratio (Table 2), we found that the decay branching ratio is smaller when considering the resonance effect. The results with and without resonance effects were compared

for the PQCD and FAT approaches. In general, owing to the lack of non-perturbation contribution and $1/m_b$ power correction, the attenuation amplitude and phase extracted from the experimental data by the FAT approach are larger than those from the PQCD or QCDF approaches, resulting in a larger decay branching ratio result. The PQCD approach only considers the decay branching ratio of $\bar{B}_s^0 \to \rho P \to \pi^+\pi^- P$ in the direct decay process, which is close to our result without considering the resonance effect. We also found that the decay branching ratio is lower when considering resonance effects, especially for the $\bar{B}_s^0 \to \pi^+\pi^-\bar{K}^0$ process. In addition, we included the uncertainty term in the calculation results.

Generally, researchers can reconstruct the intermediate virtual particles ρ, ω, and ϕ from the final state mesons of $\pi^+\pi^-$ to experimentally measure the decay branching ratio and predicted CP asymmetry. However, it is difficult to distinguish and analyze the effect of intermediate mesons ρ and ω on the final state particle production during experiments. Therefore, it is necessary to consider the resonance effect. In experiments, the $b\bar{b}$ production cross section is extremely large and of the order of 500 μb, providing 0.5×10^{12} bottom events per year [61]. For n standard deviation signatures, the number of $B_s\bar{B}_s$ pairs required is $N_{B_s\bar{B}_s} \sim \frac{n^2}{BRA_{CP}^2}(1-A_{CP}^2)$ [62], where BR is the decay branching ratio. This equation quantifies the number of $B_s\bar{B}_s$ pair statistics required to observe CP asymmetry in the $\bar{B}_s$ decay channels at n standard deviation signatures. For the decay mode $\bar{B}_s^0 \to \pi^+\pi^-\pi^0$, the number of $B_s\bar{B}_s$ pairs is 3.40×10^{10}. For $\bar{B}_s^0 \to \pi^+\pi^-\bar{K}^0$, it is 1.18×10^8 pairs. The numbers of $B_s\bar{B}_s$ pairs required for the decays $\bar{B}_s^0 \to \pi^+\pi^-\eta$ and $\bar{B}_s^0 \to \pi^+\pi^-\eta'$ are 3.70×10^{11} and 6.17×10^{10}, respectively. We found that the number of required $B_s\bar{B}_s$ pairs ranges from 10^8 to 10^{11}. The number of $B_s\bar{B}_s$ pairs at LHCb could be approximately 10^{12} per year, which is sufficient to study the impact of the $\rho-\omega-\phi$ mixing mechanism on CP asymmetry and decay branching ratios [32, 63]. Given that the LHC continues to provide more data, research on the CP asymmetry of B mesons will reach new heights in the future. We hope that this study can provide valuable support for experimental research.

APPENDIX A: DECAY AMPLITUDE

$$\mathcal{M}\left(\bar{B}_s^0 \to \rho(\rho\to\pi^+\pi^-)\bar{K}^0\right) = \sum_{q=u,c}\frac{G_F g_{\rho\pi^+\pi^-} m_\rho \epsilon(\lambda)\cdot p_K}{s_\rho}\left\{V_{ub}V_{ud}^* f_\rho a_2 + V_{tb}V_{td}^*\left[f_K A_0^{B\to\rho}\left(a_4 - \frac{1}{2}a_{10} - \frac{3}{2}a_7 - \frac{3}{2}a_9\right)\right.\right.$$
$$\left.\left. + \frac{1}{2m_\rho\epsilon(\lambda)\cdot p_K} f_{B_s} f_K f_\rho\left(b_3(\rho,K) - \frac{1}{2}b_3^{EW}(\rho,K)\right)\right]\right\}, \tag{A1}$$

$$\mathcal{M}\left(\bar{B}_s^0 \to \omega(\omega\to\pi^+\pi^-)\bar{K}^0\right) = \sum_{q=u,c}\frac{G_F g_{\omega\pi^+\pi^-\pi^0} m_\omega \epsilon(\lambda)\cdot p_K}{s_\omega}\left\{V_{ub}V_{ud}^* f_\omega F_1^{B_s^0\to K} a_2 - V_{tb}V_{td}^*\left[f_\omega F_1^{B_s^0\to K}\left(2a_3 + 2a_5 + a_4\right.\right.\right.$$
$$\left.\left.\left. - \frac{1}{2}a_{10} + \frac{1}{2}a_7 + \frac{1}{2}a_9\right) - \frac{1}{2m_\omega\epsilon(\lambda)\cdot p_K} f_{B_s} f_K f_\omega\left(b_3(\omega,K) - \frac{1}{2}b_3^{EW}(\omega,K)\right)\right]\right\}, \tag{A2}$$

$$\mathcal{M}\left(\bar{B}_s^0 \to \phi(\phi\to\pi^+\pi^-)\bar{K}^0\right) = \sum_{q=u,c}\frac{G_F g_{\phi\pi^+\pi^-} m_\phi \epsilon(\lambda)\cdot p_K}{s_\phi}\left\{V_{tb}V_{ts}^*\left[-\sqrt{2}f_\phi F_1^{B_s^0\to K}\left(a_3 + a_5 - \frac{1}{2}a_7 - \frac{1}{2}a_9\right)\right.\right.$$
$$\left.\left. - \sqrt{2}f_K A_0^{B_s^0\to\phi}\left(a_4 - \frac{1}{2}a_{10} - a_6 O_1 + \frac{1}{2}a_8 O_1\right) - \frac{1}{\sqrt{2}m_\phi\epsilon(\lambda)\cdot p_K} f_{B_s} f_K f_\phi\left(b_3(K,\phi) - \frac{1}{2}b_3^{EW}(K,\phi)\right)\right]\right\}, \tag{A3}$$

$$\mathcal{M}\left(\bar{B}_s^0 \to \rho(\rho\to\pi^+\pi^-)\eta^{(\prime)}\right) = \sum_{q=u,c}\frac{G_F g_{\rho\pi^+\pi^-} m_\rho \epsilon(\lambda)\cdot p_{\eta^{(\prime)}}}{s_\rho}$$
$$\left\{V_{ub}V_{us}^*\left[f_\rho F_1^{B_s^0\to\eta^{(\prime)}} a_2 + \frac{1}{2m_\rho\epsilon(\lambda)\cdot p_{\eta^{(\prime)}}} f_{B_s} f_\rho f_{\eta^{(\prime)}}^u (b_1(\eta^{(\prime)},\rho) + b_1(\rho,\eta^{(\prime)}))\right]\right.$$
$$\left. - V_{tb}V_{ts}^*\left[f_\rho F_1^{B_s^0\to\eta^{(\prime)}}\left(\frac{3}{2}a_7 + \frac{3}{2}a_9\right) + \frac{1}{2m_\rho\epsilon(\lambda)\cdot p_{\eta^{(\prime)}}} f_{B_s} f_\rho f_{\eta^{(\prime)}}^u\left(\frac{3}{2}b_4^{EW}(\eta^{(\prime)},\rho) + \frac{3}{2}b_4^{EW}(\rho,\eta^{(\prime)})\right)\right]\right\}, \tag{A4}$$

$$\mathcal{M}\left(\bar{B}_s^0 \to \omega(\omega \to \pi^+\pi^-)\eta^{(\prime)}\right) = \sum_{q=u,c} \frac{G_F g_{\omega\pi^+\pi^- m_\omega \epsilon(\lambda)\cdot p_{\eta^{(\prime)}}}}{s_\omega} \left\{ V_{ub}V_{us}^* \left[f_\omega F_1^{B_s^0\to\eta^{(\prime)}} a_2 + \frac{1}{2m_\omega \epsilon(\lambda)\cdot p_{\eta^{(\prime)}}} f_{B_s} f_\omega f_{\eta^{(\prime)}}^u (b_1(\eta^{(\prime)},\omega) + b_1(\omega,\eta^{(\prime)})) \right] - V_{tb}V_{ts}^* \left[f_\omega F_1^{B_s^0\to\eta^{(\prime)}} \left(2a_3 + 2a_5 + \frac{1}{2}a_7 + \frac{1}{2}a_9 \right) + \frac{1}{2m_\omega \epsilon(\lambda)\cdot p_{\eta^{(\prime)}}} f_{B_s} f_\omega f_{\eta^{(\prime)}}^u (b_4(\eta^{(\prime)},\omega) + b_4(\omega,\eta^{(\prime)}) + \frac{1}{2}b_4^{EW}(\eta^{(\prime)},\omega) + \frac{1}{2}b_4^{EW}(\omega,\eta^{(\prime)})) \right] \right\}, \tag{A5}$$

$$\mathcal{M}(\bar{B}_s^0 \to \phi(\phi \to \pi^+\pi^-)\eta^{(\prime)}) = \sum_{q=u,c} \frac{G_F g_{\phi\pi^+\pi^- m_\phi \epsilon(\lambda)\cdot p_{\eta^{(\prime)}}}}{s_\phi} \left\{ V_{ub}V_{us}^* f_{\eta^{(\prime)}}^u A_0^{B_s^0\to\phi} a_2 - V_{tb}V_{ts}^* \left[f_{\eta^{(\prime)}}^u A_0^{B_s^0\to\phi} \left\{ 2a_3 - 2a_5 - \frac{1}{2}a_7 + \frac{1}{2}a_9 + \left\{ a_3 - a_5 + a_4 - \frac{1}{2}a_{10} + \frac{1}{2}a_7 - \frac{1}{2}a_9 - (a_6 - \frac{1}{2}a_8)O_2^{(\prime)}(1 - \frac{f_{\eta^{(\prime)}}^u}{f_{\eta^{(\prime)}}^s}) \right\} \frac{f_{\eta^{(\prime)}}^s}{f_{\eta^{(\prime)}}^u} \right\} + f_\phi F_1^{B_0^s\to\eta^{(\prime)}}(a_3 + a_5 + a_4 - \frac{1}{2}a_{10} - \frac{1}{2}a_9 - \frac{1}{2}a_7) + \frac{1}{\sqrt{2}m_\phi \epsilon(\lambda)\cdot p_{\eta^{(\prime)}}} f_{B_s} f_\phi f_{\eta^{(\prime)}}^s (b_3(\eta^{(\prime)},\phi) + b_3(\phi,\eta^{(\prime)}) - \frac{1}{2}b_3^{EW}(\eta^{(\prime)},\phi) - \frac{1}{2}b_3^{EW}(\phi,\eta^{(\prime)}) + b_4(\eta^{(\prime)},\phi) + b_4(\phi,\eta^{(\prime)}) - \frac{1}{2}b_4^{EW}(\eta^{(\prime)},\phi) - \frac{1}{2}b_4^{EW}(\phi,\eta^{(\prime)})) \right] \right\}, \tag{A6}$$

The forms of the coupling constant g and parameter O in this paper are as follows:

$$g_{\rho^0\pi\pi}^2 = \frac{48\pi}{\left(1 - \frac{4m_\pi^2}{m_\rho^2}\right)^{3/2}} \times \frac{\Gamma_{\rho^0\to\pi^+\pi^-}}{m_\rho}, \quad O_1 = \frac{2m_{K^0}^2}{(m_b + m_s)(m_d + m_s)}, \quad O_2^{(\prime)} = \frac{2m_{\eta^{(\prime)}}^2}{(m_b + m_s)(m_s + m_s)}. \tag{A7}$$

APPENDIX B: INPUT PARAMETER

Table B1. Input parameter values (GeV) [6, 24, 29, 56, 64].

$\lambda_{CKM} = 0.22650 \pm 0.00048$	$A_{CKM} = 0.790^{+0.017}_{-0.012}$	$\bar{\rho}_{CKM} = 0.141^{+0.016}_{-0.017}$	$\bar{\eta}_{CKM} = 0.357 \pm 0.01$
$m_{B_s^0} = 5.36692 \pm 0.00010$	$m_\rho = 0.77526 \pm 0.00023$	$m_\omega = 0.78266 \pm 0.00013$	$m_\phi = 1.019461 \pm 0.000016$
$f_\omega = 0.192 \pm 0.010$	$f_\rho = 0.213 \pm 0.011$	$f_\phi = 0.225 \pm 0.011$	$f_{B_s} = 0.23 \pm 0.03$
$f_\pi = 0.130 \pm 0.001$	$f_K = 0.155 \pm 0.004$	$f_{\eta^{(\prime)}}^q = (1.07 \pm 0.02) f_\pi$	$f_{\eta^{(\prime)}}^s = (1.34 \pm 0.06) f_\pi$
$A_0^{B_s^0\to\phi} = 0.272$	$F_1^{B_s^0\to K} = 0.31$	$F_1^{B_s^0\to\eta_{s\bar{s}}} = 0.335$	$F_1^{B_s^0\to\eta_{s\bar{s}}^{(\prime)}} = 0.282$

References

[1] N. Cabibbo, Phys. Rev. Lett. **10**, 531 (1963)
[2] M. Kobayashi and T. Maskawa, Prog. Theor. Phys. **49**, 652 (1973)
[3] T. M. Yan, H. Y. Cheng, C. Y. Cheung *et al.*, Phys. Rev. D **46**, 1148 (1992)
[4] J. J. Qi, X. H. Guo, Z. Y. Wang *et al.*, Phys. Rev. D **99**, 076010 (2019)
[5] S. H. Zhou, R. H. Li, Z. Y. Wei *et al.*, Phys. Rev. D **104**, 116012 (2021)
[6] A. Ali, G. Kramer, Y. Li *et al.*, Phys. Rev. D **76**, 074018 (2007)
[7] R. Aaij *et al.* (LHCb Collaboration), Phys. Rev. Lett. **112**, 011801 (2014)
[8] R. Aaij *et al.* (LHCb Collaboration), Phys. Rev. D **90**, 112004 (2014)
[9] J. P. Lees *et al.* (BABAR Collaboration), Phys. Rev. D **96**, 072001 (2017)
[10] M. Wirbel, B. Stech, and M. Bauer, Z. Phys. C **29**, 637 (1985)
[11] M. Bauer, B. Stech, and M. Wirbel, Z. Phys. C **34**, 103 (1987)
[12] M. Beneke, G. Buchalla, M. Neubert *et al.*, Phys. Rev. Lett.

83, 1914 (1999)
[13] M. Beneke, J. Rohrer, and D. Yang, Nucl. Phys. B **774**, 64 (2007)
[14] H. Y. Cheng and K. C. Yang, Phys. Rev. D **78**, 094001 (2008)
[15] Y. Y. Keum, H. N. Li, and A. I. Sanda, Phys. Rev. D **63**, 054008 (2001)
[16] Y. Y. Keum and H. N. Li, Phys. Rev. D **63**, 074006 (2001)
[17] C. D. Lu, K. Ukai, and M. Z. Yang, Phys. Rev. D **63**, 074009 (2001)
[18] C. W. Bauer, D. Pirjol, and I. W. Stewart, Phys. Rev. Lett. **87**, 201806 (2001)
[19] C. W. Bauer, D. Pirjol, and I. W. Stewart, Phys. Rev. D **65**, 054022 (2002)
[20] H. Y. Cheng, C. W. Chiang, and A. L. Kuo, Phys. Rev. D **91**, 014011 (2015)
[21] X. G. He, Y. J. Shi, and W. Wang, Eur. Phys. J. C **80**, 359 (2020)
[22] X. G. He and W. Wang, Chin. Phys. C **42**, 103108 (2018)
[23] N. M. Kroll, T. D. Lee, and B. Zumino, Phys. Rev. **157**, 1376 (1967)
[24] S. Navas *et al.* (Particle Data Group), Phys. Rev. D **110**, 030001 (2024)
[25] G. Lü, Y. L. Zhao, L. C. Liu *et al.*, Chin. Phys. C **46**, 113101 (2022)
[26] M. Bander, D. Silverman, and A. Soni, Phys. Rev. Lett. **43**, 242 (1979)
[27] D. S. Shi, G. Lü, Y. L. Zhao *et al.*, Eur. Phys. J. C **83**, 345 (2023)
[28] S. H. Zhou, X. X. Hai, R. H. Li *et al.*, Phys. Rev. D **107**, 116023 (2023)
[29] X. L. Yuan, G. Lü, N. Wang *et al.*, Chin. Phys. C **47**, 113101 (2023)
[30] G. Lü, C. C. Zhang, Y. L. Zhao *et al.*, Chin. Phys. C **48**, 013103 (2024)
[31] J. M. Blatt and V. F. Weisskopf, *Theoretical Nuclear Physics*, (New York: Springer, 1952).
[32] R. Aaij *et al.* (LHCb Collaboration), Phys. Rev. D **101**, 012006 (2020)
[33] P. D. Ruiz-Femen´ıa, A. Pich, and J. Portol´es, Nucl. Phys. B Proc. Suppl. **133**, 215 (2004)
[34] M. N. Achasov, V. M. Aulchenko, A. V. Berdyugin *et al.*, Nucl. Phys. B **569**, 158 (2000)
[35] C. E. Wolfe and K. Maltman, Phys. Rev. D **80**, 114024 (2009)
[36] C. E. Wolfe and K. Maltman, Phys. Rev. D **83**, 077301 (2011)
[37] H. B. O'Connell, A. W. Thomas, and A. G. Williams, Nucl. Phys. A **623**, 559 (1997)
[38] S. Gardner and H. B. O'Connell, Phys. Rev. D **57**, 2716 (1998)
[39] M. Beneke and M. Neubert, Nucl. Phys. B **675**, 333 (2003)
[40] G. Buchalla, A. J. Buras, and M. E. Lautenbacher, Rev. Mod. Phys. **68**, 1125 (1996)
[41] D. S. Du, H. J. Gong, J. F. Sun *et al.*, Phys. Rev. D **65**, 094025 (2002)
[42] D. S. Du, J. F. Sun, D. H. Yang *et al.*, Phys. Rev. D **67**, 014023 (2003)
[43] J. J. Qi, Z. Y. Wang, Z. H. Zhang *et al.*, Phys. Rev. D **111**, 016017 (2025)
[44] C. Wang, R. W. Wang, X. W. Kang *et al.*, Phys. Rev. D **99**, 074017 (2019)
[45] H. Q. Liang and X. Q. Yu, Phys. Rev. D **105**, 096018 (2022)
[46] H. Y. Cheng, C. W. Chiang, and C. K. Chua, Phys. Lett. B **813**, 136058 (2021)
[47] M. Z. Yang and Y. D. Yang, Phys. Rev. D **62**, 114019 (2000)
[48] J. F. Sun, G. H. Zhu, and D. S. Du, Phys. Rev. D **68**, 054003 (2003)
[49] T. Muta, A. Sugamoto, and Y. D. Yang, Phys. Rev. D **62**, 094020 (2000)
[50] S. Leupold and M. F. M. Lutz, Eur. Phys. J. A **39**, 205 (2009)
[51] Z. H. Zhang, Y. D. Yang, X. H. Guo *et al.*, Eur. Phys. J. C **73**, 2555 (2013)
[52] Z. H. Zhang, X. H. Guo, and Y. D. Yang, Phys. Rev. D **87**, 076007 (2013)
[53] C. Wang, Z. H. Zhang, Z. Y. Wang *et al.*, Eur. Phys. J. C **75**, 1 (2015)
[54] C. Wang, L. L. Liu, and X. H. Guo, Phys. Rev. D **96**, 056002 (2017)
[55] B. El-Bennich, A. Furman, R. Kaminski *et al.*, Phys. Rev. D **79**, 094005 (2009)
[56] J. Chai, S. Cheng, and W. F. Wang, Phys. Rev. D **103**, 096016 (2021)
[57] O. Leitner, X. H. Guo, and A. W. Thomas, Eur. Phys. J. C **31**, 215 (2003)
[58] T. Feldmann, P. Kroll, and B. Stech, Phys. Rev. D **58**, 114006 (1998)
[59] Y. Li, A. J. Ma, W. F. Wang *et al.*, Phys. Rev. D **95**, 056008 (2017)
[60] H. Y. Cheng, C. W. Chiang, and C. K. Chua, Phys. Rev. D **103**, 036017 (2021)
[61] V. A. Khoze, A. D. Martin, and M. G. Ryskin, Eur. Phys. J. C **48**, 467 (2006)
[62] D. s. Du, Phys. Rev. D **34**, 3428 (1986)
[63] R. Aaij *et al.* (LHCb Collaboration), JHEP **03**, 047 (2025)
[64] X. L. Yuan, G. Lü, N. Wang *et al.*, Chin. Phys. C **49**, 023101 (2025)